Supplemental Figure Legends:

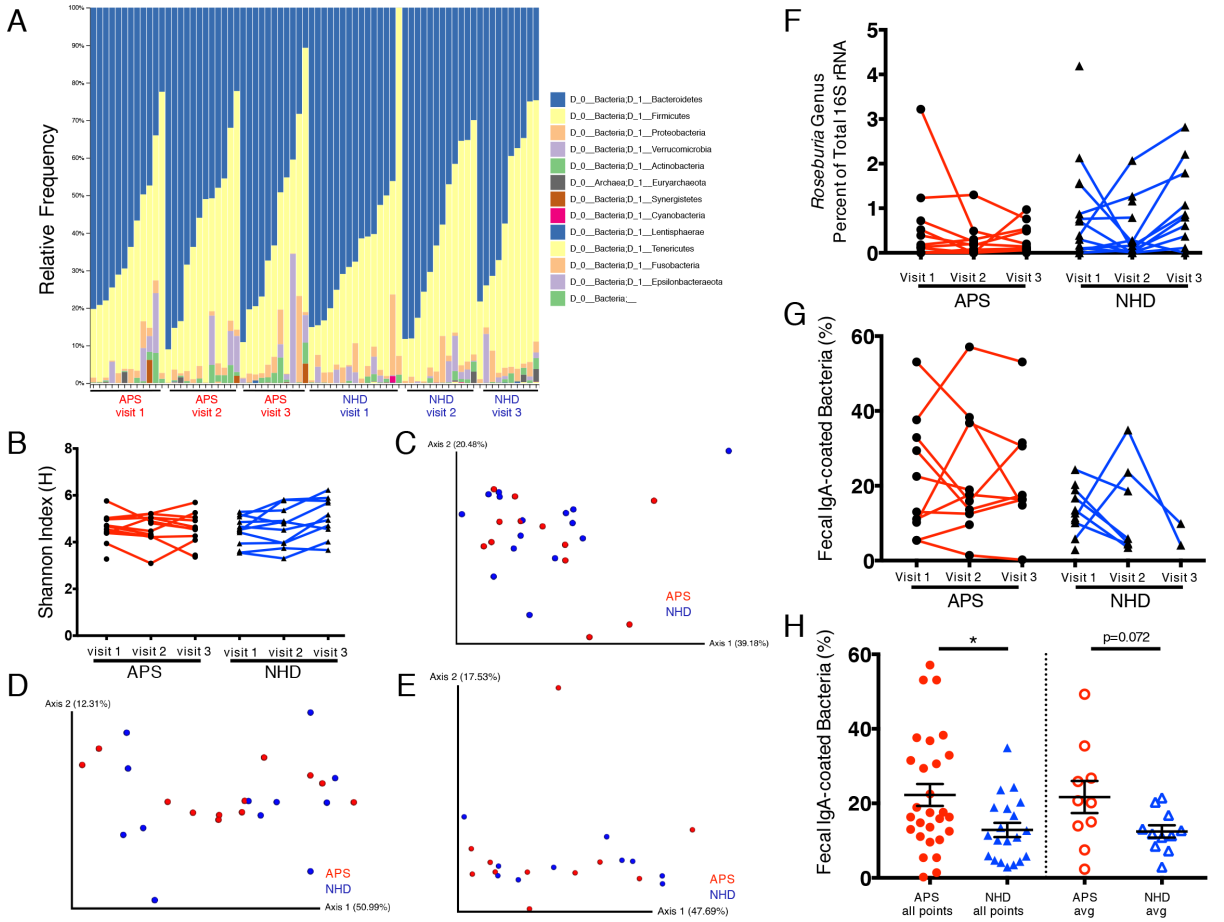

Figure S1. Related to figure 1: **No overt gut microbial dysbiosis but contracted diversity of IgA-coated gut bacteria in APS**

16S rRNA analysis performed as described in STAR Methods at a read depth of 7091 sequences per sample (APS, visit 1 n = 12, visit 2 n = 12, visit 3 n = 11; NHD, visit 1 n = 15, visit 2 n = 12, visit 3 n = 10). (A) Taxonomic bar plot showing phyla of individual fecal microbiomes. (B) Alpha diversity by Shannon-Weiner diversity index at each visit and (C-E) beta diversity as shown by weighted UniFrac distances of visit 1 (C), visit 2 (D), and visit 3 (E). (F) Relative abundance of *Roseburia* genus as a percentage of total 16S rRNA reads at each visit. (G-H) Fecal IgA coating percentages determined by FACS analysis of IgA^+ populations relative to total bacteria sorted (APS, visit 1 n = 10, visit 2 n = 10, visit 3 n = 8; NHD, visit 1 n = 11, visit 2 n = 7, visit 3 n = 2). Longitudinal (G) and individual (H) IgA coating percentages per visit or patient, respectively, are shown. Increased IgA coating occurs in APS patients compared to NHD (all time points, p = 0.038, average time points, p =0.0720). All points, all time points; avg, average; APS, antiphospholipid syndrome; NHD, normal healthy donors. Two–tailed Mann-Whitney U test performed for inter-group comparison and two-tailed Wilcoxon signed-rank test performed for intra-group comparison. Error bars represent ±SEM. *p < 0.05.

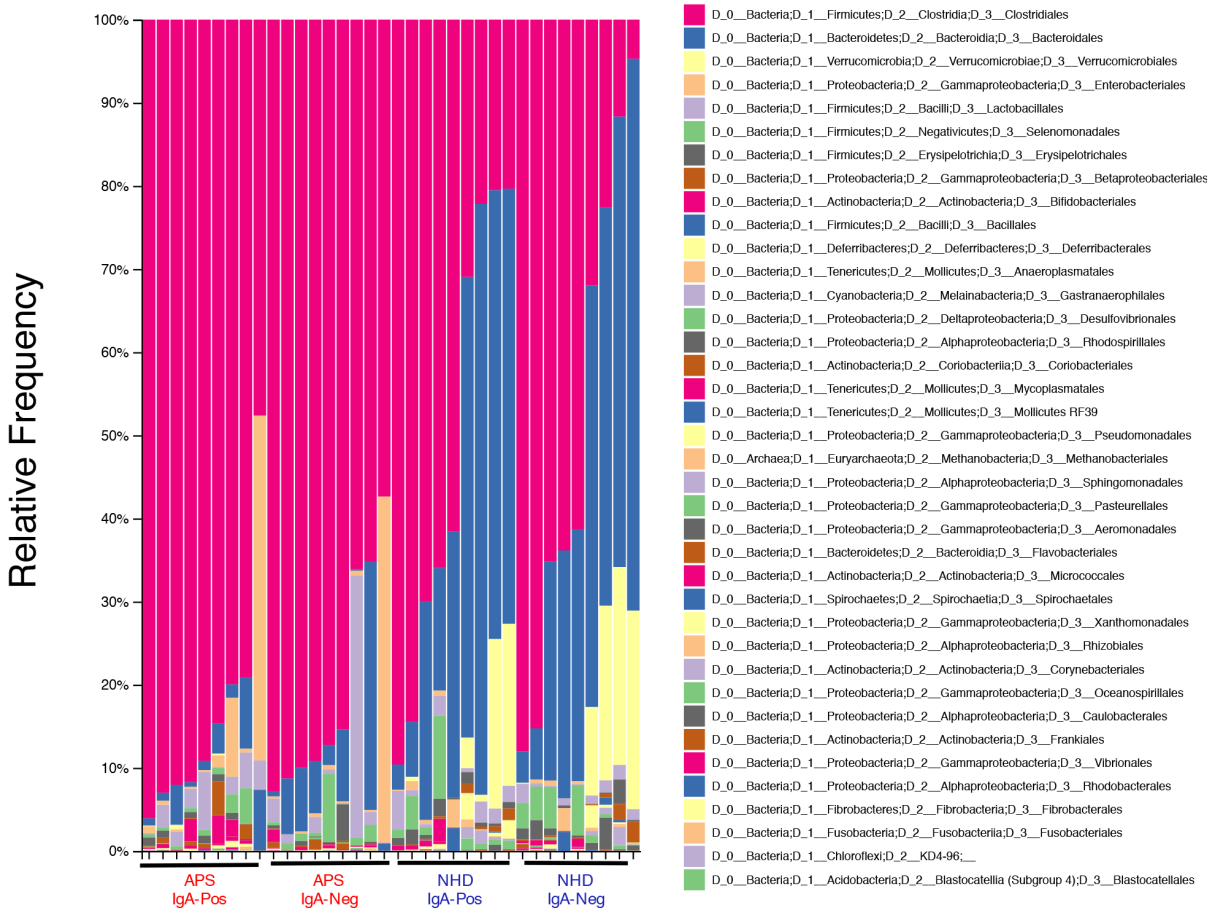

Figure S2. Related to figure 1: **IgA-seq analysis of IgA-coated gut bacteria in APS and NHD** IgA-seq analysis was performed as described in STAR Methods at a read depth of 5528 sequences per samples. Shown are individual samples at the order level. Legend shows taxa in descending order from most abundant at the top to least abundant order. APS (n = 9) NHD (n = 9). APS, antiphospholipid syndrome; NHD, normal healthy donors.

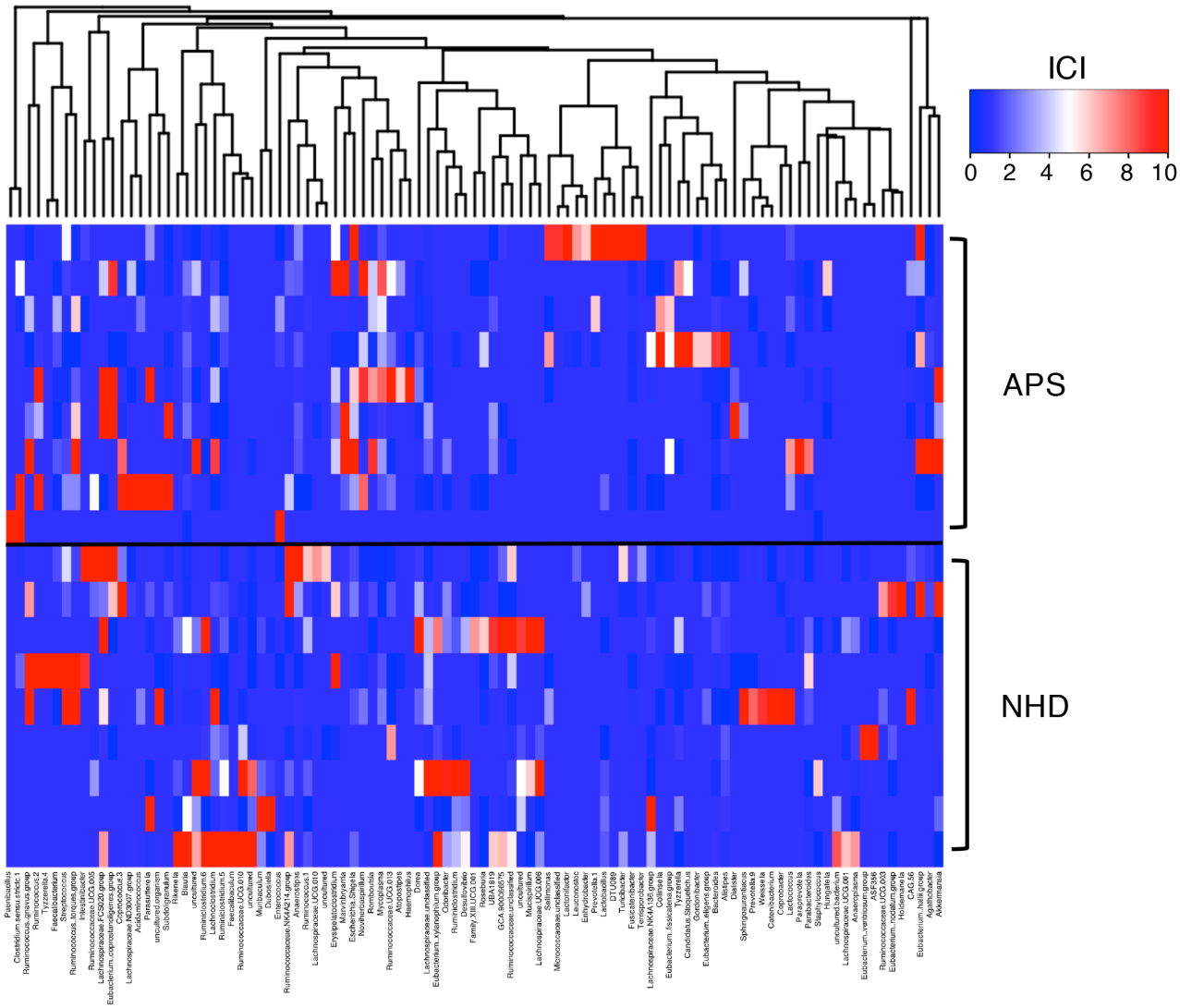

Figure S3. Related to figure 1: **IgA coating index of IgA-coated gut bacteria in APS and NHD** IgA coating index (ICI) was calculated by dividing the percentage of IgA^+ taxa by the percentage of IgA^- taxa (Palm et al., 2014). ICI heat map showing genera that had a minimum ICI of six in at least one sample. Rows represent individual subjects. APS (n = 9) NHD (n = 9). APS, antiphospholipid syndrome; NHD, normal healthy donors. Hierarchical clustering of taxa was performed using Bray Curtis Similarity.

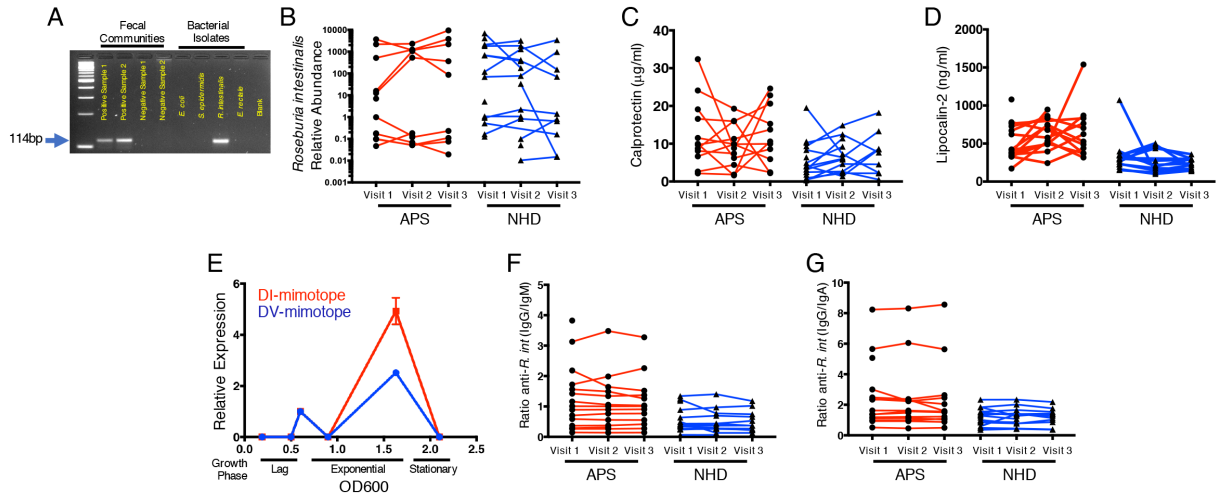

Figure S4. Related to figure 1: ***R. int* relative abundances, gut and peripheral inflammation, and systemic anti-*R. int* antibody responses across time**

(A) Primers targeting a non-16S rRNA gene specific to *R. intestinalis* (*R. int*) were designed using Primer BLAST. Primers were validated to be specific by end-point PCR. Positive control 1 and 2 are human fecal DNA samples positive for *Roseburia* genus by 16S rRNA sequencing. Negative control 1 and 2 are human fecal DNA samples containing microbiomes negative for *Roseburia* genus by 16S rRNA sequencing. Pure cultures of *Escherichia coli* (*E. coli*), *Staphylococcus epidermidis* (*S. epidermidis*), *Eubacterium rectale* (*E. rectale*), and *Roseburia intestinalis* (*R. intestinalis*) are used as individual strain controls with *E. rectale* being phylogenetically closest to *R. int*. (B) Loads of *R. int* relative to total 16S rRNA by fecal DNA PCR were not significantly different between APS and NHD (APS, visit 1 n = 15, visit 2 n = 15, visit 3 n = 14; NHD, visit 1 n = 20, visit 2 n = 16, visit 3 n = 12. (C-D) Fecal calprotectin (C) and plasma lipocalin-2 (D) levels were determined by commercially available ELISAs. Individuals taking proton pump inhibitors and regular NSAIDs were excluded from calprotectin analysis. Fecal calprotectin (APS, visit 1 n = 12, visit 2 n = 12 visit 3 n = 11; NHD, visit 1 n = 18, visit 2 n = 13, visit 3 n = 9) and plasma lipocalin-2 (APS, visit 1 n = 15, visit 2 n = 13, visit 3 n = 12; NHD, visit 1 n = 17, visit 2 n = 13, visit 3 n = 13) do not change significantly across time. (E) A growth curve analysis of *R. int* L1-82 was performed using OD_{600} as a readout of growth. *R. intestinalis* L1-82 reaches stationary phase around OD_{600} 2.0. qPCR primers specific for the β_2GPI p276-290 mimic-containing gene and β_2GPI domain I R39-43 mimic-containing gene were used to determine gene expression levels. Values are relative to gene expression at OD_{600} 0.6. Both the p276-290 and R39-43 mimic are highest expressed at OD_{600} 1.63. (F-G) Plasma anti-*R. int* IgG/IgM (F) and IgG/IgA (G) ratios were determined as described in STAR Methods and were stable over time (APS, visit 1 n = 17, visit 2 n = 14 visit 3 n = 13; NHD, visit 1 n = 17, visit 2 n = 14, visit 3 n = 12). APS, antiphospholipid syndrome; NHD, normal healthy donors. Two–tailed Mann-Whitney U test performed for inter-group comparison and two-tailed Wilcoxon signed-rank test performed for intra-group comparison.

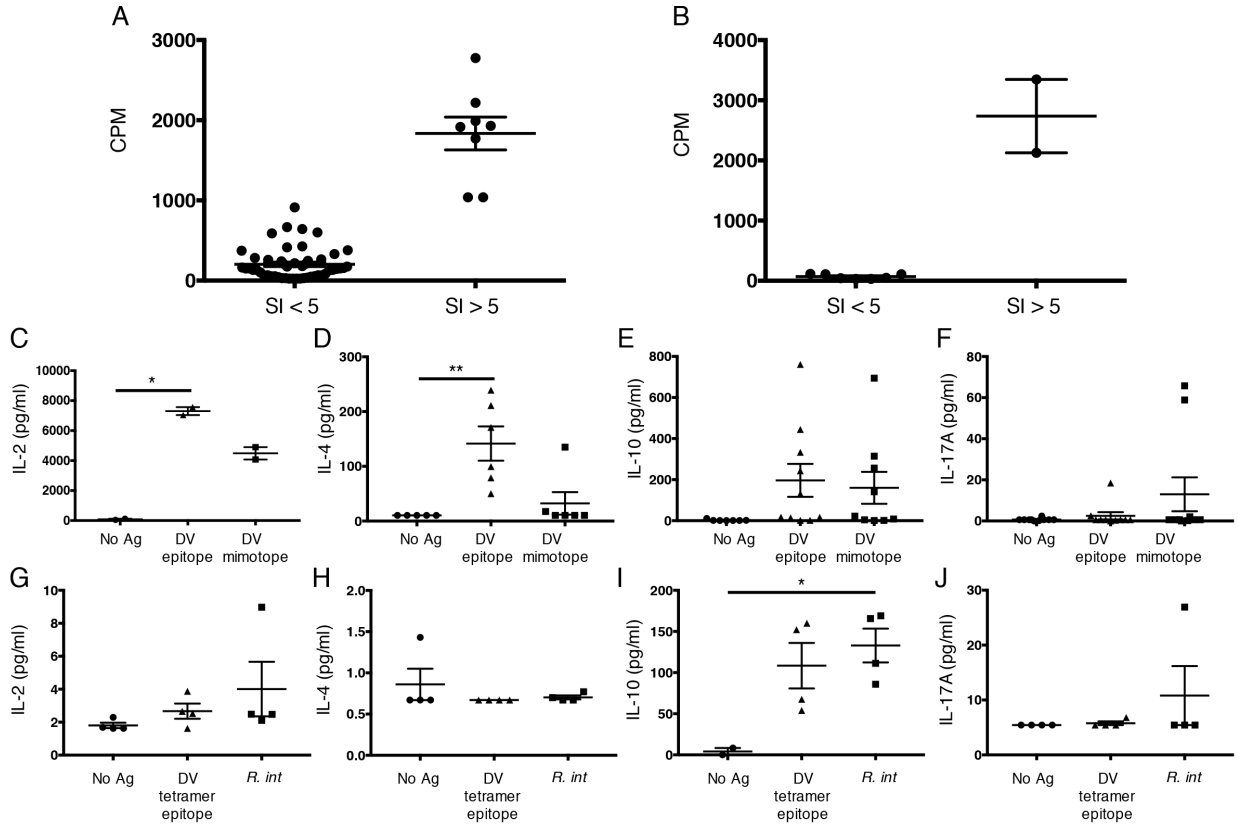

Figure S5. Related to figure 2: **Proliferation and cytokine secretion patterns of human β_2GPI-reactive APS-derived memory T cell clones cross-reactive with *R. int* mimotope**

(A-F) Human APS patient memory T cells were sorted into CD45RA$^-$, CD45RO$^+$, CD25$^-$ β_7^+ CCR6$^-$ (A) and CCR6$^+$ (B) subsets and stimulated with rhβ_2GPI. Counts per minute (CPM) were measured by ^{3}[H]-thymidine incorporation. Stimulation index (SI) was calculated as CPM of stimulated clones divided by CPM of unstimulated clones. Each point on the graph represents one clone. Eight clones from the gut-homing (integrin $\beta7^+$) CCR6$^-$ subset (A) had an SI $\geq$ 5 compared to only two from the CCR6$^+$ subset (B). (C-F) Clones were re-stimulated with 100 μg/ml β_2GPI p276-290 peptide (DV epitope), *R. int* p276-290 mimotope (DV mimotope), or no antigen (Ag), respectively. Supernatants were collected 72 hours after in vitro culture and measured using a bead-array assay. Cytokine values for IL-2 (C), IL-4 (D), IL-10 (E), and IL-17A (F), respectively, are shown. (G-J) Cytokine values from human tetramer-positive CD45RA$^-$ CD45RO$^+$ CD25$^-$ clones re-stimulated as in Figure 2D are shown for IL-2 (G), IL-4 (H), IL-10 (I), and IL-17A (J), respectively. Unpaired, two-tailed Student's t-test. Error bars represent ±SEM. *p < 0.05, **p < 0.01, ***p < 0.001, ****p < 0.0001.

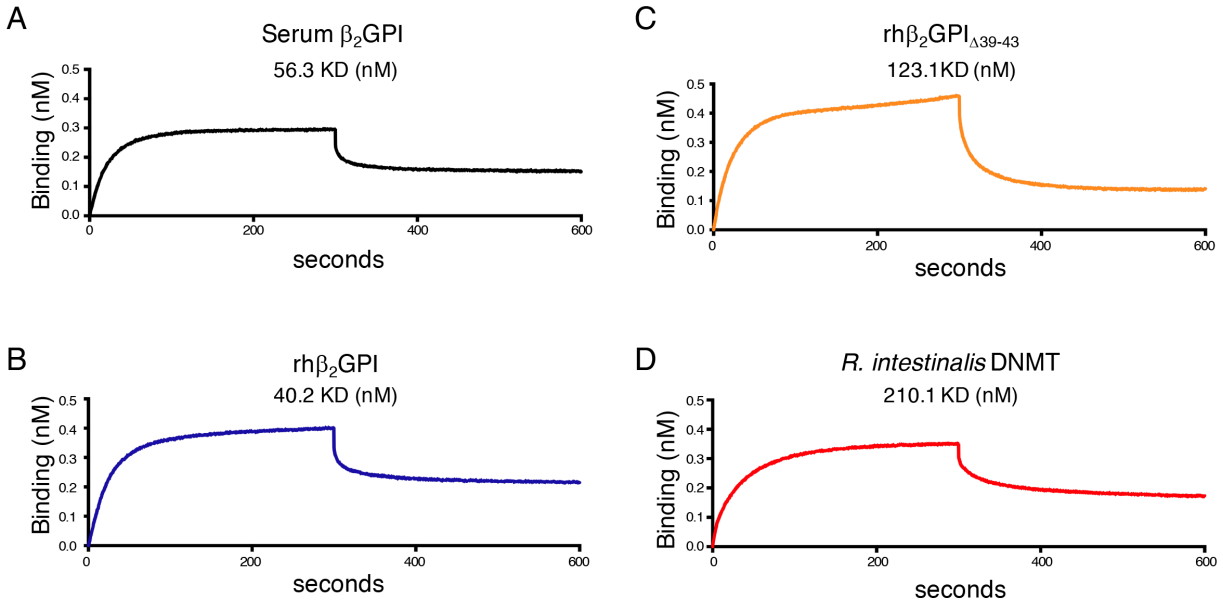

E

Antibody	Analyte	KD (nM)	ka (1/Ms)	kd (1/s)
P1-117	serum-derived β_2GPI	56.3	2.80E+05	1.58E-02
P1-117	rhβ_2GPI	40.2	5.82E+05	2.34E-02
P1-117	rhβ_2GPI$_{\Delta 39\text{-}43}$	123.1	2.38E+02	3.04E-02
P1-117	*R. intestinalis* DNMT	210.1	1.59E+04	1.19E-02
P1-117	rhInsulin	5800	1.41E+04	1.97E-02

Figure S6. Related to figure 3: **Anti-β_2GPI mAb P1-117 equilibrium dissociation constants** Bio-layer interferometry sensorgrams were obtained using anti-human IgG Fc biosensors (ForteBio) loaded with 10 μg/ml of P1-117. Binding to serum-derived β_2GPI, rhβ_2GPI, rhβ_2GPI$_{\Delta 39\text{-}43}$, recombinant *R. int* DNMT, and recombinant human insulin (rhInsulin) was determined for each protein. Each analyte was tested in a dilution series of 200 nM, 100 nM, 50 nM, 25 nM, and 0 nM of analyte. Binding curves were fit globally to a 1:1 binding model in order to yield equilibrium dissociation constant (K_D). Representative sensorgram data from P1-117 interacting with 200 nM serum-derived β_2GPI (A), with 200 nM rhβ_2GPI (B), with 200 nM rhβ_2GPI$_{\Delta 39\text{-}43}$ (C), and with 200 nM *R. int* DNMT (D). (E) Equilibrium dissociation constant (K_D), and association (k_a), and dissociation (k_d) constants are shown for each analyte including the unrelated autoantigen insulin.

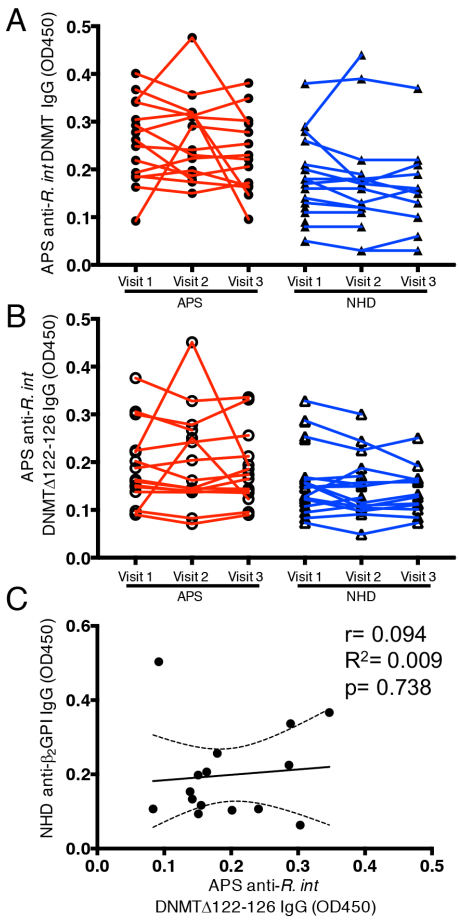

Figure S7. Related to figure 4: **Anti-*R. int* DNMT and anti-*R. int* DNMT$_{\Delta 122\text{-}126}$ IgG levels in the systemic circulation of APS patients and NHDs over time**

ELISAs for *R. int* DNMT and *R. int* DNMT$_{\Delta 122\text{-}126}$ IgG antibodies in the plasma of APS (APS, visit 1 n = 15, visit 2 n = 15 visit 3 n = 14) and NHDs (NHD, visit 1 n = 20, visit 2 n = 16, visit 3 n = 12). Plasma was diluted 1:1000 from all samples in the study cohort and probed for IgG. (A) Anti-*R. int* DNMT IgG levels do not significantly change across time in APS and NHD in most subjects. (B) Anti-*R. int* DNMT$_{\Delta 122\text{-}126}$ IgG values levels do not significantly change across time. (C) Average APS anti-*R. int* DNMT$_{\Delta 122\text{-}126}$ IgG levels (x-axis) do not correlate with increasing average anti-β_2GPI IgG autoantibodies (y-axis). Two-tailed Pearson, r=0.094, R^2=0.009, p = 0.738. APS, antiphospholipid syndrome; NHD, normal healthy donor. Two-tailed Wilcoxon signed-rank test.

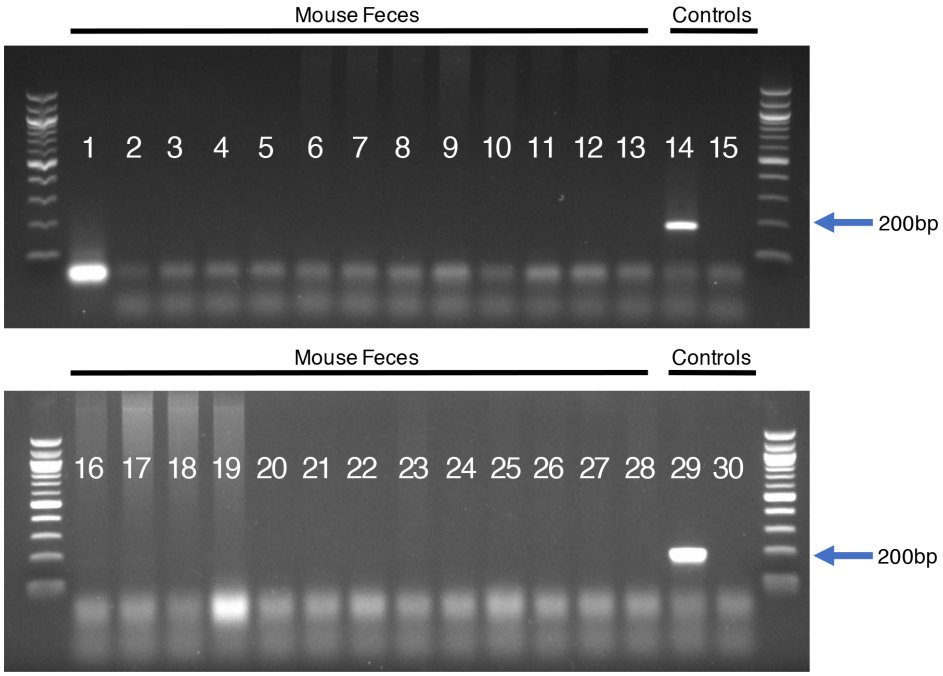

Figure S8. Related to Figure 6: **Vancomycin treatment depletes *Enterococcus gallinarum*** Representative murine stool screening for *Enterococcus gallinarum* by PCR performed as previously described (Manfredo Vieira et al., 2018). *E. gallinarum* species-specific PCRs of DNA from (NZW x BXSB)F_1 mouse feces (samples 1 – 13 and 16-28, treated with vancomycin for 2 weeks starting at 4-6 weeks of age). *E. gallinarum* DNA (samples 14 and 29) and water (samples 15 and 30) served as positive and negative controls, respectively. The size for the *E. gallinarum* PCR product is 173 bp.

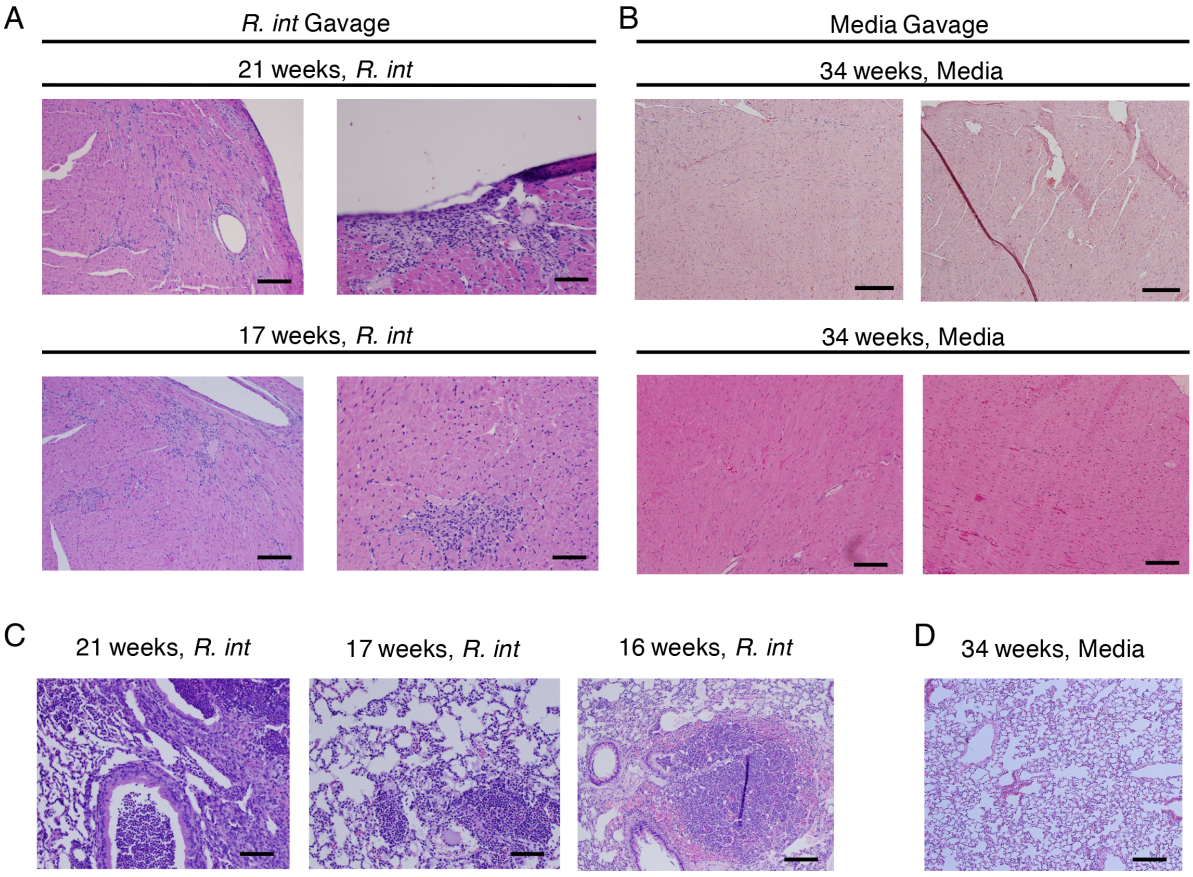

Figure S9. Related to Figure 6: **Oral gavage with *R. int* induces autoimmune pathology in male (NZW x BXSB)F_1 mice**

(A) (NZW x BXSB)F_1 mice gavaged with *R. int* show widespread myocardial and subendocardial lymphocytic infiltrates after APS-related mortality occurring at 21 weeks (upper panel) and 17 weeks (lower panel), respectively. (B) Control (NZW x BXSB)F_1 mice gavaged with media that survived until 34 weeks, at which time they were euthanized, showed unremarkable myocardium without any evidence of inflammation (representative micrographs of H&E-stained myocardium from 2 separate mice, upper panel and lower panel, respectively). (C) Mice gavaged with *R. int* succumbed to APS-related deaths at 21, 17 and 16 weeks of age, respectively, with signs of inflammation in the lungs (representative micrographs of H&E-stained lung tissues are shown). Diffuse lymphocytic infiltrates and rare granuloma formation were visible. Mild vascular changes were noted as well, however, definitive thrombi were not identified. (D) All control (NZW x BXSB)F_1 mice gavaged with media only (representative image of one mouse shown) had unremarkable airspaces without evidence of inflammation or thrombosis. Scale bar = 500 μm.

Table S1. Related to table 1: **Additional cohort information**

α-Cardiolipin, anti-cardiolipin IgG (- (negative) < 20.0 chemiluminescent units (CU), + (positive) > 20.0 CU); LA, lupus anticoagulant; ANA, anti-nuclear antibody titer (-(negative) < 1:80, +(positive) > 1:80); C3, complement 3 (low < 81 mg/dL, normal 81 - 145 mg/dL, high > 145 mg/dL); C4, complement 4 (low < 16 mg/dL, normal 16 - 39 mg/dL, high > 39 mg/dL; PPI, proton pump inhibitor; NSAIDs, nonsteroidal anti-inflammatory drugs; BMI, body mass index, QD, once a day; BID, twice a day; NA, not assessed.